CORE
Metadata, citation and similar papers at core.ac.uk
Provided by Qucosa - Publikationsserver der Universität Leipzig

Spatial variability of temperature and wind over heterogeneous surfaces

K. Arnold, A. Ziemann, A. Raabe and G. Spindler

Abstract

Conventional micro-meteorological measuring methods are not particularly suitable for the investigation of the energy exchange under heterogeneous surface conditions. To consider the influence of the different surface properties, area-covered and spatially averaged meteorological measurements in combination with highly resolved simulations are necessary. In this context, the method of acoustic travel time tomography is introduced to provide information about the horizontal temperature and wind field.
Within a field experiment (STINHO-1; Melpitz 2001) the tomographic system and conventional meteorological equipment were utilised inside the investigation area with an extension of several hundred meters (300×700 m^2), which was arranged over areas with different surface properties: grassland and bare soil.
The results of the field experiment show that differences between the measuring systems (in-situ and remote sensing) exist and the heterogeneity of the underlying surface is visible in the near surface temperature and wind field at a scale, which can be resolved with highly resolved numerical models. Depending on the incoming solar radiation and the local advection regional distinctions in the air temperature and wind field as well as in the vertical sensible heat fluxes were observed.
The investigations demonstrate that the sensitivity of the Acoustic Tomography is sufficient to verify gradients in the meteorological fields even when the horizontal differences are small.

Zusammenfassung

Zur Untersuchung des Energieaustausches über heterogenem Gelände sind konventionelle mikro-meteorologische Messungen und Modellvorstellungen allein nicht ausreichend. Um den Einfluss unterschiedlicher Oberflächen besser berücksichtigen zu können, sind flächendeckende und räumlich mittelnde meteorologische Messungen kombiniert mit hoch aufgelösten numerischen Simulationen notwendig. In diesem Kontext wird die Methode der Akustischen Laufzeitomographie vorgestellt, mit der horizontale Wind- und Temperaturfelder in geeigneter Weise bereitgestellt werden können.
Im Rahmen eines Feldexperimentes (STINHO-1; Melpitz 2001) wurde das tomographische System zusammen mit konventionellen meteorologischen Geräten in einem Untersuchungsgebiet mit einer Ausdehnung von mehreren hundert Metern (300×700 m^2) über unterschiedlichen Oberflächen (Wiese und gepflügter Acker) eingesetzt.

Die Ergebnisse des Feldexperimentes zeigen, dass Unterschiede zwischen den einzelnen Messverfahren existierten und die Heterogenität der Unterlage in den oberflächennahen Temperatur- und Windfeldern auf einer Skala sichtbar ist, die mit kleinskaligen numerischen Modellen aufgelöst werden kann. Die vorgestellten Untersuchungen demonstrieren, dass die Sensitivität der Akustischen Tomographie hinreichend ist, um Gradienten meteorologischer Felder auch bei geringeren horizontalen Unterschieden nachzuweisen.

1. Introduction

Spatially averaged data have been conventionally provided by point measurements and additional interpolation or up-scaling algorithms. A relatively new way to obtain such values directly and with a high spatial and temporal resolution is the application of tomographic meth-

ods in the atmospheric surface layer. Here we use a type of acoustic travel time tomography where the sound speed can be determined by measuring the travel time of a signal at a defined propagation path. Applying a suitable procedure, measurements of the speed of sound can be used to reconstruct horizontal temperature and wind velocity fields. (ARNOLD et al., 1999; RAABE et al., 2000; ZIEMANN et al., 2001; TETZLAFF et al., 2002).

Up to now the Acoustic Tomography was used to provide temperature fields with a maximum range of approx. 200 to 300 m^2, under rough assumptions for the wind influence. For this study the tomographic array had to be enlarged in order to observe the influence of the inhomogeneous investigation area. Also the tomographic procedure had to be enhanced to supply independent spatial temperature and wind information.
The field experiment STINHO (**ST**ructure of the turbulent fluxes under **INHO**mogeneous surface conditions) in autumn 2001 was the first comprehensive attempt to arrange the tomographic array over a real landscape with different land-use types. The tomographically and conventionally measured results showed that due to the variable surface conditions horizontal gradients in the temperature and wind field developed.
Subsequent examinations should clarify, how these heterogeneous surface conditions influence the vertical sensible heat flux. These investigations should lead to a better understanding of the energy exchange above micro-scale heterogeneous surfaces.

2. Tomographic reconstruction technique

Tomography is applied as a measurement and an imaging technique, which provides a cross-section of the investigated area using the response of the medium of an external energy source. Spatial information about the investigated medium results from the inversion of all single line integrals between emitters and receivers (MUNK et al., 1995; WILSON et al., 2001).
The application of this technique to the atmosphere takes advantage of the facts that (1) the travel time of an acoustic signal between transmitter and receiver is a function of the actual meteorological conditions and (2) the atmosphere is roughly transparent to low-frequency sound, so that signals can be principally transmitted over distances of some hundred meters (TETZLAFF et al., 2002).
When this technique is transferred to the turbulent atmosphere, one prerequisite – constant properties during the exploration time – is hardly guaranteed. However, the successful application to the atmosphere was demonstrated in horizontal-slice schemes by SPIESBERGER and FRISTRUP (1990) and WILSON and THOMSON (1994) and in vertical-slice schemes by, e.g., CHUNCHUZOV et al. (1990).
In contrast to these studies ARNOLD et al. (1999), RAABE et al. (2001) and ZIEMANN et al. (1999) demonstrated the applicability of acoustic travel time tomography to detect absolute values of meteorological quantities (temperature and wind vector) without additional information apart from air humidity.

2.1 Derivation of temperature and wind data

To prepare data for tomographic application it is necessary to separate the coupled influences on the effective sound speed, which are the air temperature, the humidity and the wind vector. As first simplification the specific humidity was assumed as horizontally uniform and determined by additional measurements with standard sensors. To distinguish between the temperature and wind influence in this study we used for the first time the bi-directional sound propagation between several sound sources and receivers that were arranged perpendicular. Analogous to a sonic anemometer (see e.g. KAIMAL and GAYNOR, 1991) the wind components along the propagation path in both orthogonal directions as well as the sound speed c_L were determined independently (ARNOLD et al., 2003).

The thus obtained spatial distribution of the wind field is called '(wind-) tomogram'. The following recalculation of the spatial distribution of the air temperature field, by use of a tomographic reconstruction technique, provides the tomogram of the (acoustic virtual) temperature. This procedure is documented in detail in ZIEMANN et al. (1999) and RAABE et al. (2001).

2.2 Accuracy of the method

The data accuracy depends on several factors: the travel time and the sound path length determination, the signal processing, the separation technique, the environmental conditions as well as the quality of the tomographic reconstruction (ARNOLD, 2000; ARNOLD et al., 2001; ZIEMANN et al., 2002).
The measuring accuracy itself depends on the travel time determination as well as on the ascertainment of the ray path length between sources and receivers. The actual travel time accuracy amounts to about ± 0.3 milliseconds and a sound path determination to about ± 10 cm. The ray-path approximation affects both the direct travel-time analysis and the tomographic data reconstruction. For an error estimation regarding the straight-ray-path approximation the meteorological conditions were considered using the vertical sound speed gradient. With increasing sound speed gradient (depending on the vertical temperature and wind profile), the ray paths are curved stronger and the deviation from the linear path increases likewise (ARNOLD, 2000). The error made by this approximation was also quantitatively estimated using a sound-ray model including a generalized equation of refraction (cf. ZIEMANN et al., 2001). In summary, the straight-line approximation can be applied if we use path lengths of sound rays not more than some hundred meters over a relatively homogeneous surface, and if moderate vertical temperature and wind gradients are present.
With the actual measuring accuracy and for a source receiver distance of more than 200 m an exactness of the air temperature of ± 0.5 K and for the wind speed of ± 0.5 ms^{-1} for one time step and as spatial mean is reachable, for shorter distances the error increases correspondingly (ARNOLD, 2000). A substantial decrease of the measuring inaccuracy is possible if the single measurements are temporally averaged. For instance with a repetition rate of one minute and an averaging interval over 10 minutes the measuring accuracy amounts to $\pm 0.5\ K / \sqrt{10} \approx 0.2$ K for the temperature, respectively.
However, there remains an uncertainty due to the influence of the separation of the temperature and wind vector on the sound speed.

3. Experimental Set-up

Within the framework of the VERTIKO network project (German Research Ministry funding – AFO2000) the field experiment STINHO was carried out in autumn 2001. The aims of the STINHO experiment were to determine the horizontal divergence of the sensible heat flux over heterogeneous surfaces and to verify the representativeness of point measurements for the surrounding area.
For the STINHO experiment the research station of the Institute for Tropospheric Research (IfT) in Melpitz (51°32' N, 12°54' E, 86 m a.s.l.) was used. The IfT research station is situated near the village Melpitz in the vicinity of the city of Torgau (river Elbe valley). The station is located on a flat 100-years-old meadow surrounded by agricultural land. For further information see SPINDLER et al. (2001).
The investigation area with an extension of $300 \times 700\ m^2$ was arranged over a region with two typical different surface properties: one part was grassland (meadow) and the other was bare soil (recently tilled arable crop). Thus, due to the different vegetation properties and depending on the radiation conditions, horizontal differences in the air temperature field were expected.

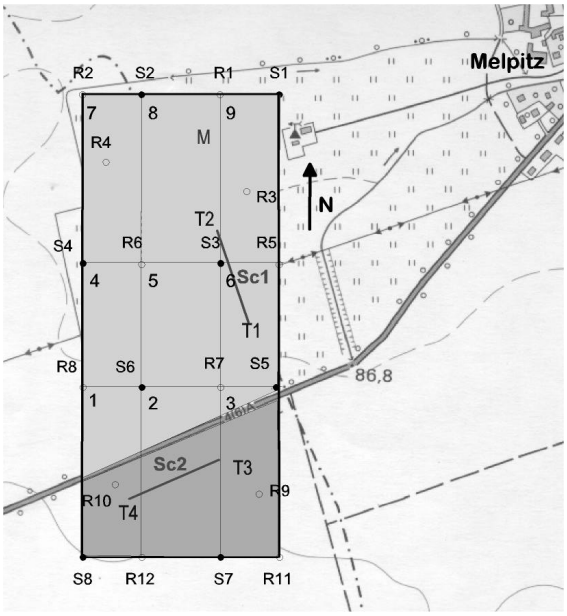

Figure 1: Layout of the area under investigation (300 × 700 m^2) at the research station Melpitz. The northern part of the array was grassland and southerly of the road was bare soil. The number 1 to 9 represent the wind cells, the receivers are labelled R1 to R12, the sources S1 to S8. T1 to T4 are the humitter sensors, Sc1 and Sc2 the scintillometer and M the routinely working 12 m profile mast.

Several measuring systems were utilized during the field experiment to compare the tomographic data set with in-situ measurements. In addition to the acoustic travel time tomography two scintillometer (Scintec SLS20) were used to provide horizontal line averaged turbulent heat fluxes. Supplementary conventional point measurements of temperature und humidity were carried out at four different points inside the array with humitter sensors (humidity – temperature probes (pt100) inside ventilated shelters). A 12 m wind (cup anemometer) and temperature (psychrometer) profile mast from the research station was also used for comparison with the tomographic data set.

Figure 1 illustrates the layout of the investigation area and the tomographic array. For the acoustic system twelve sound sources and eight receivers were positioned at the borders or inside the array. The positions of the transmitters and receivers were set in such a way that the coverage of the investigation area with sound paths is optimal and a bi-directional sound propagation between different pairs of transducers is ensured.

The large extension of the tomographic array affected that not all source-receiver connections can be used for the analysis. To ensure a roughly straight-ray sound propagation and for a practical signal/noise ratio only path lengths below 400 m (1.2 s travel time) were considered. Therefore, the number of possible sound paths is 62 (instead of 96 paths).
With these 62 sound speed line integrals and the mentioned extension of the investigation field, area averaged values for the air temperature can be provided for 32 grid cells (100 × 100 m^2). The temperature grid cells were arranged in such a way that all boxes overlap the borders of the measuring field with a half grid cell width (50 m). Due to the number of transmitter and receiver pairs the wind vector can be determined for 9 cells with an extension of 90…100 × 180…260 m^2. The size of the wind cells depends on the distance between each transducer pair, whereby all pairs inside the array pertain also to the adjoining cell and the cells clash at the border.
The repetition interval is technically limited by the data transfer rate. Due to the data volume, we used a repetition rate of 1 min for the acoustic measurements.

4. Experimental Results

To present some results from the STINHO experiment, one sunny day during the measuring campaign with low wind speed from the South, the 06.10. 2001, was selected. This day was

chosen because the local variability of the meteorological parameters can be observed over longer periods, owing to the absence of mesoscale advection.
After separating the humidity influence, which was determined with the humitter sensors, the wind speed and direction inside the 9 cells (see fig. 1) were calculated using reciprocal sound propagation. As another result, the air temperature distribution for the 32 grid cells can be calculated with the tomographic algorithm.
Figure 2 provides examples for combined temperature/wind tomograms. These pictures show a horizontal slice of 30 min averaged temperature and wind field at a height of 2 m above the ground at different times. Due to the temporal averaging over 30 minutes the accuracy increases and amounts to 0.2 K for the temperature, 0.2 ms^{-1} for the wind speed and 30° for the wind direction (ARNOLD et al., 2003) The legend represents the actual range and the resolution of the temperature field. One can detect spatial differences in the air temperature and in the wind field above the investigated area. About noon (12:30 - 13:00 local time, left side), the slightly increasing wind speed (2 - 3 ms^{-1}) from southerly directions causes a well-mixed temperature field. The observed temperature variances (for averaged values) are less than 1 K. During the cooling in the evening the wind speed decreases and temperature differences between the grassland (northern part) and the bare soil (southern part) are visible. Between 20:15 and 20:45 local time (fig. 2, right side), the wind speed decreases below 1 ms^{-1} and the direction varies inside the array, concurrent temperature differences up to 2 K between the colder grass and the warmer bare soil were observed.

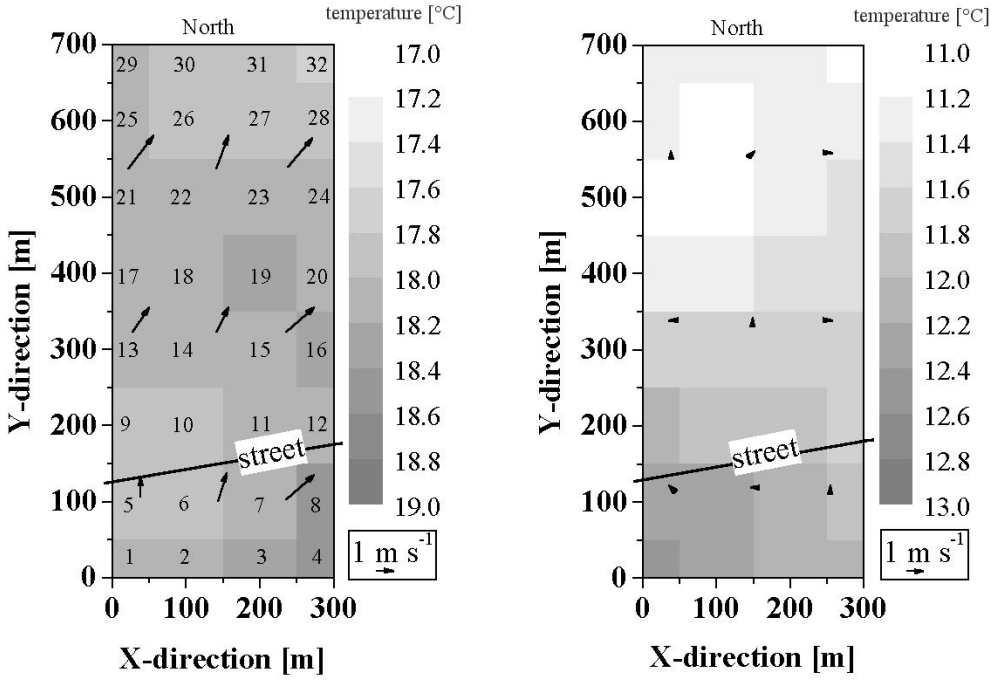

Figure 2: Horizontal slice (30 min averaged values) through the temperature (grey-scale) and wind (arrows) field at a height of 2 m above the ground on 06. 10. 2001; left side: 12:30- 13:00 local time, right side 20:15-20:45 local time. The straight line marks a street and the separation between grassland (northern part) and bare soil (southern part). The legend indicates the actual range and the achievable resolution of the temperature as well as for the wind vector. The numbers on the left tomogram (1… 32) represent the temperature cells.

To evaluate the acoustically estimated data, they were compared with the conventional in-situ measurements, which were located inside the tomographic array. As a result area-averaged tomographic data were compared with point measurements carried out with the humitter sensors and profile mast.

Figure 3 and 4 shows the comparison of ten-minute averaged temperature and wind values between the Acoustic Tomography and the in-situ measurements, all at approximately 2 m above the ground. This comparison shows the meteorological conditions on the selected day and at the same time the capability of the acoustic tomographic monitoring. This sunny day was characterised by a strong warming up in the morning (from approx. 5 °C to 20 °C) and low wind speed during the whole day. In the evening during the cooling phase an advection of warmer air masses is also visible. This local advection, which is combined with increasing wind speed from the South, transports warmer air from the surrounding wood.
The acoustic temperature data represent the 24 cells (see fig. 2) above grassland and six cells above bare soil (two cells were not considered due to the mixed surface conditions).
For the determination of the wind speed and direction above grass six cells (4 to 9 in fig. 1) were used.
Figures 3 and 4 demonstrate the differences of the measuring systems and the influence of the underlying surface. Especially concerning day temperature (fig. 3) clear deviations between the tomography and the humitter sensors are visible. During nighttime remarkable differences between the temperature above grassland and bare soil are signed out for both measuring systems with the same sign and amplitude: warmer air temperatures were observed above the bare soil. Whereas during the day, the variances between the land-use types decreases and differences between the measuring systems increase. During the day air temperatures observed with the humitter sensors are generally warmer then retrieved by tomography, above grassland and bare soil as well.

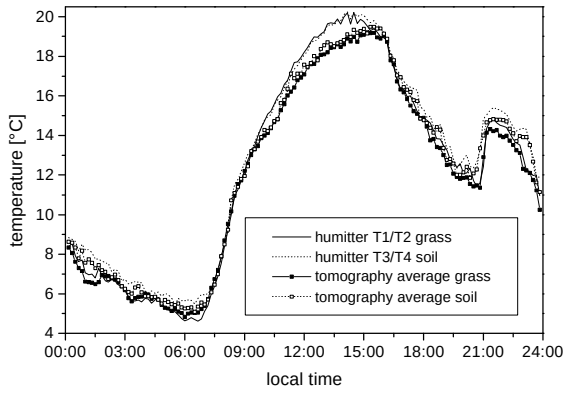

Figure 3: Diurnal course of air temperature above different vegetation types on the 06.10. 2001. Comparison of the 10-minute average values of a) Acoustic Tomography: above grassland (cells 9…32) and bare soil (cells 1…4, 7, 8) and b) humitter above grassland (T1/T2) and bare soil (T3/T4).

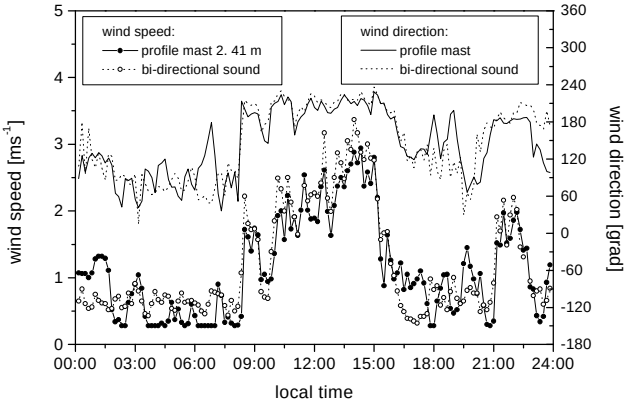

Figure 4: Diurnal course of wind speed and direction above grassland on the 06.10.2001. Comparison of the 10-minute average values of bi-directional sound propagation and profile mast.

Figure 4 show that in-situ as well as the acoustic wind speed and direction measurements provide approximately the same values, whereby on this day only low wind speed conditions with the highest values at midday were observed. Minor deviations of the wind direction were only observed during low wind speed periods. One reason for the apparent distinctions between the wind speed measurements at night is the inertia (threshold: 0.28 ms^{-1}) of the cup anemometer.

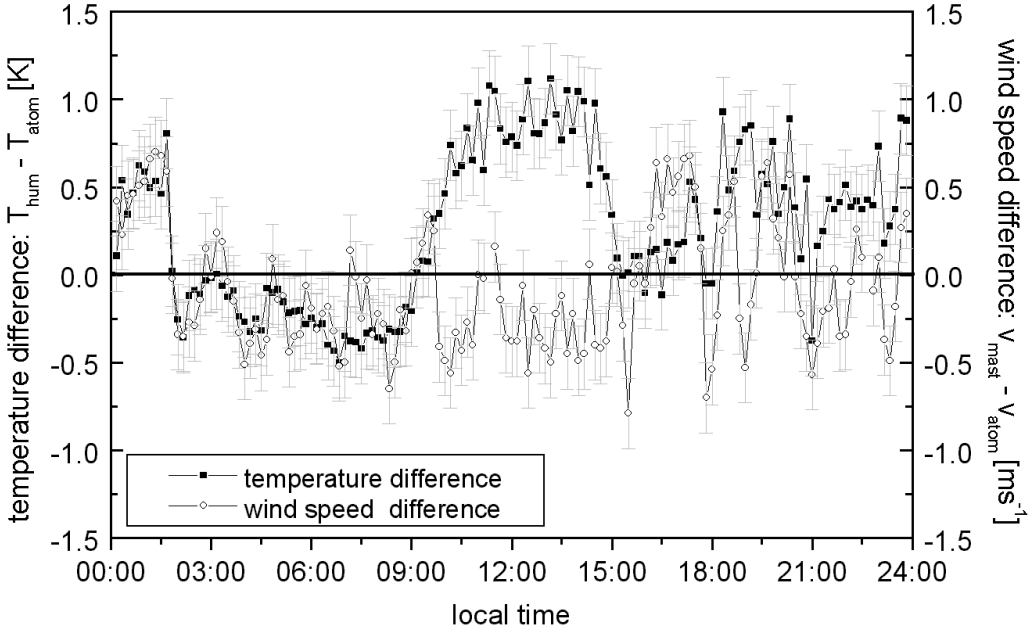

Figure 5: Diurnal course of the difference in air temperature and wind speed above grassland on the 06.10.2001, measured by different methods. Difference between conventional and acoustic measurements in 10-minute average values of temperature: $T_{hum} - T_{atom}$ and wind speed: $v_{hum} - v_{atom}$. The error bars indicate the uncertainness range of Acoustic Tomography.

Deviations between the instruments are more distinct if instead of its absolute values differences between them are directly shown. Therefore, in figure 5 as an example the deviations between the measuring systems above grassland are plotted for the temperature and wind speed as well. To indicate the significance of this comparison error bars of the acoustically derived values are added. Considering a temporal averaging of 10 minutes and additional a spatial averaging the error of the Acoustic Tomography amounts to 0.2 K for the temperature and approx. 0.2 ms^{-1} for the horizontal wind speed.

Figure 5 show that several hours the independent measurements provide nearly the same air temperature than tomography (deviations smaller than ± 0.5 K). However, depending on the incoming solar radiation significant differences in air temperature measurements were observed. Especially during the daytime conditions (from 09:00 to 15:00 local time) the temperature was overestimated by the humitter due to the influence of the direct solar radiation, despite the fact that sensors are installed inside a ventilated shelter. A similar result was derived using data from a previous experiment (Lindenberg-experiment 1999, see: e.g. ZIEMANN et al., 2002).

The observed distinctions in the horizontal wind speed are a hint of an inaccurateness of the separation algorithm and spatial varieties inside the area under investigation (ARNOLD et al., 2003). For the evaluation of these measuring instruments, we have to consider, that point measurements were compared with values, which were spatially integrated over up to several hundred meters. Therefore, the variances inside the tomographic array due to local heterogeneities (also above grassland) and the slope of the terrain (the incline of the grassland site is approx. 1 m per 500 m) affect the tomographic measurements.

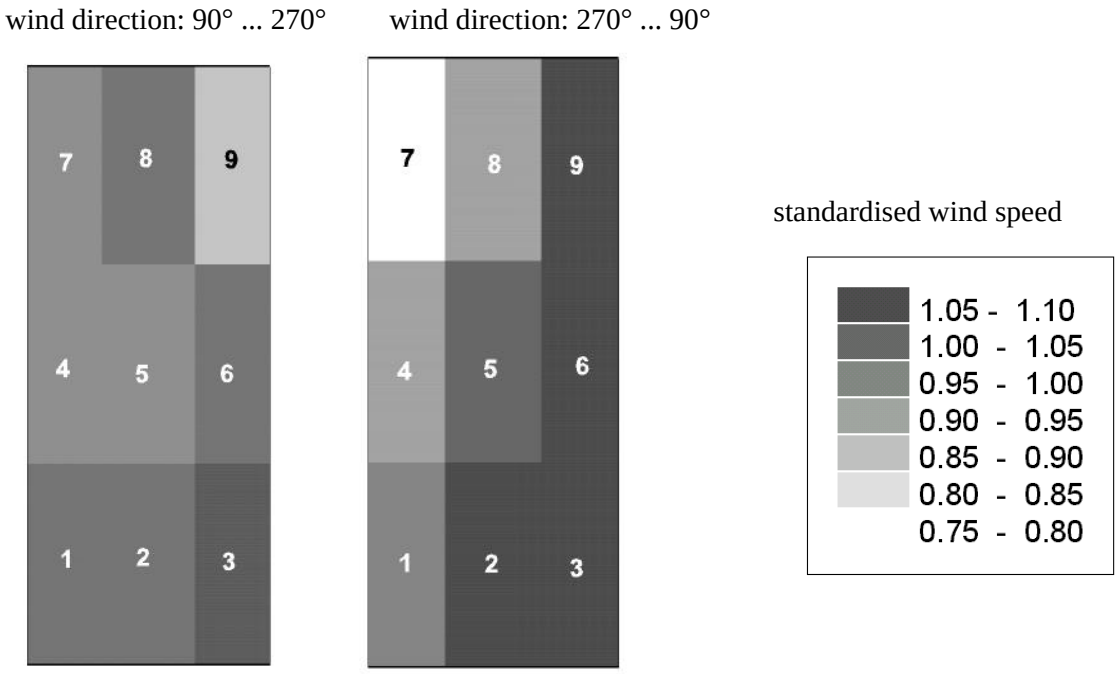

Figure 6: Deviation of the horizontal wind speed inside the nine wind cells (fig. 1) form the mean wind velocity depending on the prevailing wind direction on 06.10.2001. The left side contains all data (wind speed > 0.5 ms^{-1}) with wind from southern directions (90°... 270°), the right side are all values with northern wind (270°... 90°) directions (dimensions of the tomographic array and wind cells see fig.1 and 2).

In Figure 6 the spatial deviation from the mean value of the wind speed inside the cells are shown. The variations of the horizontal wind field change depending on the prevailing wind direction. To ensure a reasonably uniform wind direction and sufficient accuracy here only data with wind speeds higher than 0.5 ms^{-1} were considered. For **southwards wind direction** (90 ° … 270 °; left panel of fig. 6) the spatial deviations are relatively small, only in cell 9 somewhat lower wind speeds were observed. During **wind from the North** (270 ° ... 90 °; right panel of fig. 6) the variations of the wind speed inside the investigation area are more significant. The wind speed in the cells 3, 6, and 9 on easterly side of the array is higher than in the remaining cells.
One reason for the observed behavior is, that during wind from southern directions the wind speed is higher (see fig. 4 and 7) and therefore the wind field is uniform. In the case of wind from northern directions the wind speed is very low (mostly between 0.5 and 1 ms^{-1}) and the spatial variability as well the influence of the measuring accuracy is high.

The determination of the wind vector in several cells with a practicable accuracy and spatial resolutions allows calculating the divergence of the horizontal wind field. In the demonstrated case the divergence was determined by the averaged value of all possible wind speed differences $\Delta u/\Delta x$ and $\Delta v/\Delta y$:

$$\nabla \cdot \mathrm{v}_h = \frac{\partial u}{\partial x} + \frac{\partial v}{\partial y} \cong \frac{\overline{\Delta u}}{\overline{\Delta x}} + \frac{\overline{\Delta v}}{\overline{\Delta y}} = \frac{1}{n}\sum_{i=1}^{n}\frac{\Delta u_i}{\Delta x_i} + \frac{1}{n}\sum_{i=1}^{n}\frac{\Delta v_i}{\Delta y_i},$$

which can be retrieved from the grid structure shown e.g. in figure 1.

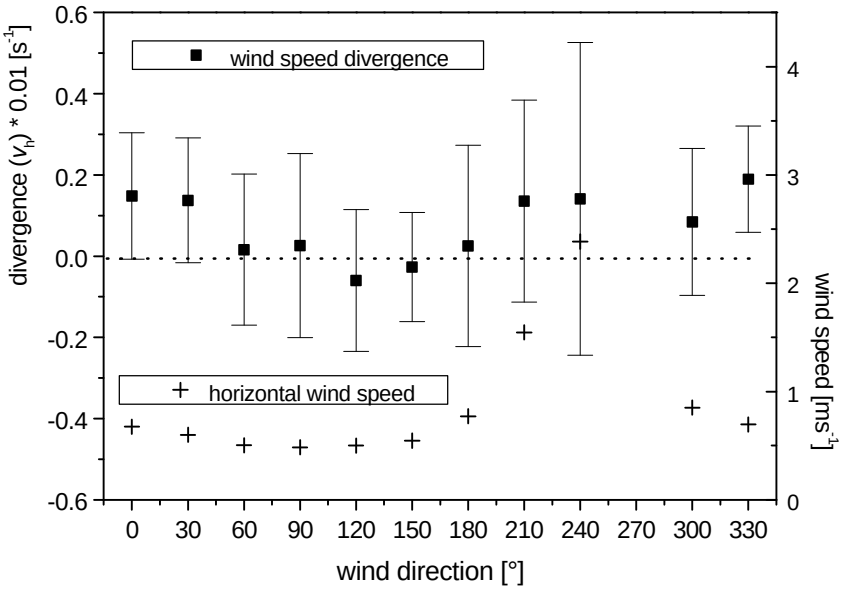

Figure 7: Divergence of the horizontal wind speed (upper curve) and averaged horizontal wind speed of the nine cells (lower curve) depending on the wind direction on 06.10.2001. For the divergence only values with wind speeds > 0.5 ms^{-1} were considered. The error bars marks the range of the standard deviation of the divergence.

Figure 7 shows, that the divergence (which includes the directional and velocity component) including the error bars inside this small array depends on the wind speed and direction. The wind divergence increases significant at wind directions between northwest (330°) and north-east (30°) as well at southwest and is not equal zero summed over all directions, temporary the values outstand from the error range. The explanation for the observed behaviour is not simple, one reason could be that the horizontal heterogeneity of the terrain influence the wind field and causes horizontal divergences.

In the following, the influence of the heterogeneity of the underlying surface on vertical turbulent heat exchange is investigated. The method of Acoustic Tomography provides horizontal temperature distributions, which can be used to calculate temperature gradients or even horizontal turbulent fluxes by use of the gradient method. In figure 8 the tomographically derived horizontal temperature gradients were compared with the vertical sensible heat fluxes measured with the scintillometers above grassland and bare soil (Sc1 and Sc2). The horizontal temperature gradients were determined by use of the average of the temperature difference between the outer cells above bare soil (cell 1 to 4) minus the cells above grass (cell 29 to 32) divided by the distance.
This comparison shows that the horizontal temperature gradients between bare soil and grass-land are relatively small, however, occasionally they correspond with modifications in the vertical heat fluxes. Distinct differences between the vertical sensible heat fluxes over the two different surfaces (more than 10 Wm^{-2}) were observed in the morning (09:00 to 12:00 local time) and intermittently during the late evening (after 22:00 local time). During the warming up in the morning higher sensible heat fluxes were observed above the grassland. This is the opposite of the expected behaviour, because higher temperatures above the soil were observed owing to the stronger heating from the ground (see fig. 2 and 3). This result demonstrates that the near surface temperature distribution does not allow at all times to draw conclusions of the vertical sensible heat fluxes. The explanation for the observed heat flux differences over the two surfaces lies in the energy balance for each land use type. The bare soil was very wet after a longer raining period, therefore most of the energy was released in the latent heat flux.

Above the grass lower air temperatures were observed, however, due to dryer surface conditions – especially at the area around the scintillometer Sc1 – higher sensible heat fluxes were observed.

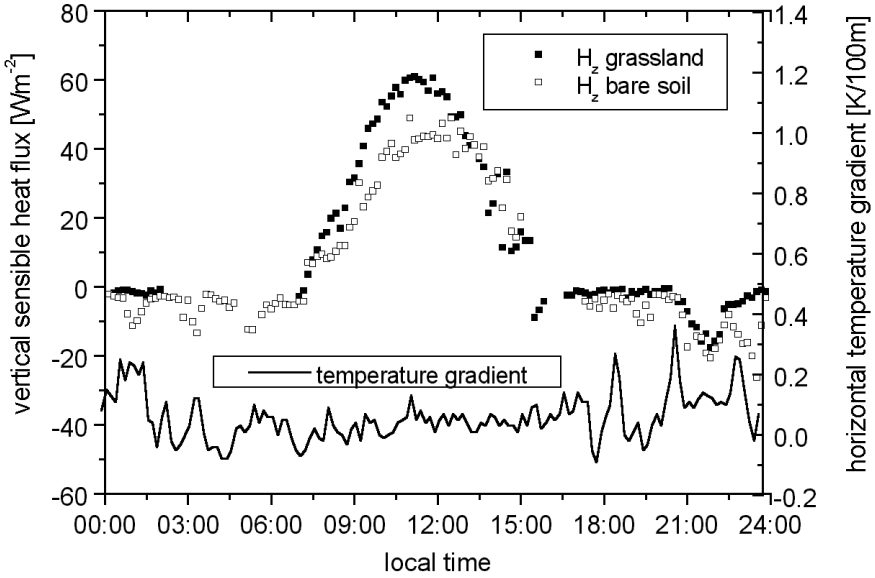

Figure 8: Diurnal course of vertical sensible heat flux (scintillometer) above grassland (Sc1) and bare soil (Sc2) and averaged horizontal temperature gradients (tomography) between the northern cells (29…32) and the southern cells (1…4).

A significant change in the vertical heat fluxes is also visible during the local heat advection in the late evening (after 21:00 local time). The warming was first observed above the bare soil, because the arable crop is closer to the surrounding wood, which is probably the origin of the warmer air.
The night time variances in the heat fluxes due to local advection corresponds with the horizontal temperature distribution, where the higher temperatures above the bare soil causes a significant temperature gradient in south–north direction.
The observed differences in the vertical sensible heat fluxes in the morning, with higher fluxes above the grassland, do not correspond with the horizontal temperature gradients, which is an indication of a well-mixed temperature field.

5. Discussion

This study demonstrates the applicability of the tomographic monitoring of near surface horizontal temperature and wind fields. Here for the first time acoustic travel time data were directly (bi-directional sound propagation) used to estimate the wind vector distribution inside the tomographic array (nine cells). Applying these results, tomographic reconstructions of air temperature distributions can be retrieved using the resulting sound speed data.
This study pointed out the limits and the potentials of the Acoustic Tomography. The applicability of this method depends on the attained accuracy, the meteorological conditions and the object of investigation. To realise an error range, which is smaller than the observed phenomena, a temporally average at least over 10 values is necessary. With these requirements the tomographic method is suitable to detect also small differences in the temperature and wind field. Especially under low wind conditions the Acoustic Tomography is excellent to apply, because no inertia of the sensors affect the measurements. Under these conditions one general problem of the tomographic procedure, the separation of the different influences on the sound speed is also negligible. Otherwise, there are no strong limits for the utilisability of the tomo-

graphy apart from technical problems like background noise (due to high wind speeds) or wetness at the microphones.
The remote sensing of area or volume averaged values is a fundamental advantage of the Acoustic Tomography. For this reason this method is applicable for the detection of heterogeneous meteorological fields, in particular in inaccessible regions like e.g. mountain valleys or above waterbodies. The use of conventional point measurements inside such heterogeneous areas cannot guarantee the coverage of the whole variability, especially of all fine structures, of the meteorological fields without making an enormous effort. Additionally the sensors itself also affect the investigated medium. Another benefit of tomography is that many more data points per sensor can be generated than with traditional techniques.

The results show that differences in the parameters are either due to different observational methods such as remote sensing systems versus in-situ measurements or due to different spatial dimensioning –area or line-averaged measurements versus point measurements. The Acoustic Tomography provides representative data for an array with a horizontal extension of 300×700 m^2, with a spatial resolution of 32 temperature (100×100 m^2) and 9 wind ($90\ldots100 \times 180\ldots260$ m^2) cells.
Depending on the respective land use type different micro-meteorological conditions were observed. Due to the difference in the surface properties, bare soil and grass, at the selected day higher air temperatures were observed above the arable land. Also within each land use type, particularly within the grassland, local inhomogeneities exist, which can be proved by the tomographic measurements.

The horizontal temperature and wind distributions, provided by the Acoustic Tomography with a repetition rate of one minute, can be used to investigate the relation between point measurements and the thermal and dynamical conditions in the surrounding area. The results of this investigation have shown that this method is applicable to verify the representativeness of point measurements for the surrounding area.
The observed horizontal temperature differences allow recalculating of gradients of the temperature field and in addition to other measurements the calculation of turbulent heat flux divergences. The presence of horizontal temperature gradients is an indicator for the violation of the assumptions (stationarity and homogeneity) made for the application of an only one-dimensional approach to quantify the vertical turbulent fluxes of sensible heat (RAABE et al., 2002).
The horizontal temperature gradients, combined with other results, will be used to estimate the amount of the horizontal divergences of the gradient sensible heat fluxes. These divergences should quantify the influence of the surface heterogeneity on energy balance measurements at one point.
Future work will be focused on the generalisation of the results and on providing parameterisations for the complex turbulent transport in the atmospheric boundary layer for numerical models, like Large-Eddy Simulations, e.g. RAASCH and HARBUSCH (2001).

Acknowledgements

Especially we acknowledge Dr. S. v. Hünerbein, Prof. S. Bradley and C. Stolle for their great interest and valuable portion at the document.
We would like to thank F. Weiße and M. Engelhorn for their support in the development and manufacturing of the acoustic measuring system. Special thanks also to Dr. Schienbein for the development and maintenance of the humitter sensors. Our spatial thanks are to T. Conrath for data preparation as well as the staff of the research site Melpitz and the students from the Leipziger Institute for Meteorology for the assistance during the field experiment.

This work was supported by the Bundesministerium für Bildung und Forschung (BmBF) under grant PT-UKF-07ATF37.

References

Arnold, K., Ziemann, A., Raabe, A., 1999: Acoustic tomography inside the atmospheric boundary layer. Phys. Chem. Earth (B) **24**, 133-137.

Arnold, K., 2000: Ein experimentelles Verfahren zur Akustischen Tomographie im Bereich der atmosphärischen Grenzschicht (in German). Wiss. Mitt. Inst. für Meteorol. Univ. Leipzig u. Inst. für Troposphärenforschg. Leipzig, **18**, 137 pp.

Arnold, K., Ziemann, A., Raabe, A., 2001: Tomographic monitoring of wind and temperature in different heights above the ground. Acustica, **87**, 703-708.

Arnold, K., Ziemann, A., Raabe, A., Spindler, G., 2003: Acoustic tomography and conventional meteorological measurements over heterogeneous surfaces. Meteorol. Atmosph. Phys. accepted.

Chunchuzov, I.P., Bush, G.A., Kulichkov, S.N., 1990: On acoustical impulse propagation in a moving inhomogeneous atmospheric layer. J. Acoust. Soc. Am., **88,** 455–461.

Kaimal, J.C., Gaynor, J.E., 1991: Another look at sonic thermometry. Boundary-Layer Meteorol., **56**, 401-410.

Munk, W., Worcester, P., Wunsch, C., 1995: Ocean acoustic tomography. Cambridge University Press, New York. 433 pp.

Raabe, A., Arnold, K., Ziemann, A., 2000: Horizontal turbulent fluxes of sensible heat and horizontal homogeneity in micrometeorological experiments. Proc. 10th Intl. Symp. Acoust. Rem. Sens., Auckland, 146-149.

Raabe, A., Arnold, K., Ziemann, A., 2001: Near surface averaged air temperature and wind speed determined by acoustic travel time tomography. Meteorol. Z., **10**, 61-70.

Raabe, A., Arnold, K., Ziemann, A., 2002: Horizontal turbulent fluxes of sensible heat and horizontal homogeneity in micrometeorological experiments. J. Atmos. Oceanic Technol., **19**, 1225-1230.

Raasch, S., Harbusch, G., 2001: An analysis of secondary circulations and their effects caused by small-scale surface inhomogeneities using Large-Eddy simulation. Boundary-Layer Meteorol., **101**, 31-59.

Spiesberger, J.L., Fristrup, K.M., 1990: Passive localization of calling animals and sensing of their acoustic environment using acoustic tomography. Am. Natural., **135**, 107-153.

Spindler, G., Teichmann, U., Sutton, M.A., 2001: Ammonia dry deposition over grassland – micrometeorological flux-gradient measurements and bidirectional flux calculation using an inferential model. Q.J.R. Meteorol. Soc., **127**, 795-814.

Tetzlaff, G., Arnold, K., Raabe, A., Ziemann, A., 2002: Area covering observations of near-surface wind and temperature fields in real terrain using Acoustic travel time tomography. Meteorol. Z., **11**, 273-283.

Wilson, D.K, Thomson, D.W., 1994: Acoustic tomographic monitoring of the atmospheric surface layer. J. Atmos. Oceanic Technol., **11**, 751-768.

Ziemann, A., Arnold, K., Raabe, A., 1999: Acoustic travel time tomography - A method for remote sensing of the atmospheric surface layer. Meteorol. Atmosph. Phys., **71**, 43-51.

Ziemann, A., Arnold, K., Raabe, A., 2001: Acoustic tomography as a method to identify small-scale land surface characteristics. Acustica **87**, 731-737.

Ziemann, A., Arnold, K., Raabe, A., 2002: Acoustic tomography as a remote sensing method to investigate the near-surface atmospheric boundary layer in comparison with in situ measurements. J. Atmos. Oceanic Technol., **19**, 1208-1215.

Addresses of Authors

K. Arnold, A. Ziemann and A. Raabe :
Institute of Meteorology, University of Leipzig, Stephanstr. 3, D-04103 Leipzig, Germany
G. Spindler:
Institute for Tropospheric Research, IfT, Permoserstr. 15, D-04318 Leipzig, Germany